# Design and Multiplierless Implementations of 9th order linear-Phase Bireciprocal Lattice Wave Digital Wavelet Filter Banks

**Jassim M. Abdul-Jabbar**
Computer Engineering, University of Mosul
College of Engineering / drjssm@yahoo.com

**Rasha Waleed Hamad**
Electrical Engineering, University of Mosul,
Rasha-Waleed87@yahoo.com

## Abstract

**In this paper, a filter bank structure for the implementation of infinite impulse response (IIR) discrete wavelet transform (DWT) is proposed. Bireciprocal lattice wave filters (BLWDFs) are utilized in a linear-phase design of 9th order IIR wavelet filter bank (FB). Each of the two branches in the structure of the BLWDF bank realizes an all-pass filter. Filters of this bank belong to the intermediate design group, maintaining linear-phase property with best roll-off characteristics in their frequency responses. The design is first simulated using Matlab7.10 programming in order to investigate the resulting wavelet filter properties and to find the suitable wordlength to represent the BLWDF's coefficients in quantized forms for best selection of some prescribed performance measures. All adopted measures show an excellent closeness to some typical cases. Each coefficient in the resulting structure is realized in a multiplierless manner after representing it as sum-of-powers-of-two (SPT). Multiplications are then achieved by only shift and add. Multiplierless FPGA implementations of the proposed IIR wavelet filter banks are also achieved with less complexity and high operating frequency.**

**Keywords: Bireciprocal Lattice Wave Filters (BLWDFs), Bireciprocal Lattice Wave Discrete Wavelet Filter Banks (BLW-DWFBs), IIR Wavelet Filter Banks, Scaling and Wavelet Functions, Linear Phase Processing, FPGA Implementations.**

# تصميم وبناءات عديمة المضارب لأجراف المرشحات المويجية من النوع الرقمي الموجي المتشابك ثنائي التبادل من المرتبة التاسعة وبطور خطي

**د. جاسم محمد عبد الجبار**
قسم هندسة الحاسوب- كلية الهندسة
جامعة الموصل- الموصل-العراق

**رشا وليد حمد**
قسم الهندسة الكهربائية - كلية الهندسة
جامعة الموصل- الموصل-العراق

## الخلاصة

**في هذا البحث أقترحت هيكلية لاجراف المرشحات لبناء التحويل المويجي المقطع من نوع IIR. لقد أستخدمت المرشحات الرقمية الموجية المتشابكة ثنائية التبادل (BLWDFs) في تصميم جرف مرشح مويجي نوع IIR من المرتبة التاسعة وبطور خطي وكان كل من القناتين في ذلك الهيكل هو من نوع BLWDF التي تحقق مرشحاً للامرار الكلي، ان المرشحات في هذا الجرف تنتمي الى مجموعة التصميم الوسيطي محافظةً على خاصية الطور الخطي مع خصائص انحدار فضلى في استجاباتها الترددية.إن التصميم تم محاكاته اولا باستخدام برنامج Matlab7.10 للتحقق من خصائص المرشحات المويجية الناتجة ولايجاد طول الكلمة المناسب لتمثيل معاملات ذلك المرشح وبصيغ مكظمة لافضل اختيار لبعض قياسات الاداء المعتمدة. واظهرت جميع القياسات المعتمدة تقارباً ممتازاً للحالات النمطية. ان كل معامل في تلك الهياكل الناتجة تم تحقيقة بدون مضارب بعد تمثيلة بطريقة (SPT). ومن ثم بنائه باستخدام عمليات الازاحه والجمع فقط. وعلية فقد تم الحصول على بناءات بأعتماد FPGA عديمة المضارب للتصميم المقترح لاجراف المرشحات المويجية نوع IIRباقل تعقيد وبتردد اشتغال عال.**

**Received: 2 – 10 - 2011** **Accepted: 22 – 11 – 2012**

## I. Introudaction

Discrete Wavelet Transform (DWT) is a powerful tool for signal processing and analysis [1]. The success of DWT stems from its ease of computation and its inherent decomposition of an image into non-overlapping subbands that enables the design of efficient algorithms and allows for incorporation of the human visual system [2]. The extension of DWT to efficient implementation of filter banks, has provided a way to efficiently utilize wavelets for signal processing [1]. Filter banks can be realized using finite impulse response (FIR) or infinite impulse response (IIR) filters. FIR filters have large transition bands. If both sharp transition band and reasonable stopband attenuation are required, one must use very high order FIR filters. In VLSI and other implementations, high order means that a large amount of multipliers are required. Lower order IIR filters can be achieved with sharp transition bands and good stopband attenuations [3]. However, linear-phase and orthonormality are not mutually exclusive properties for IIR filter banks, as they are in an FIR case[4].

In this paper, IIR wavelet filter, with perfect reconstruction and linear-phase properties is designed. The structure of this filteris based on the bireciprocal lattice wave filter (BLWDF) to simulate a two channel wavelet filter bank. BLWDF is employed in a $9^{th}$ order IIR filter to form an intermediate filter bank. The wave lattice is composed of two parallel real all-pass sections. $2^{nd}$ order to $1^{st}$ order all-pass filter section reduction method is applied via downsampling position alteration in the designed structure.Consequently, the resulting bireciprocal lattice wave discrete wavelet filter banks(BLW-DWFBs) structure possess efficient computations. Linear-phase is accomplished by laying the impulse responses of the synthesis bank filters as time-reversed versions of the analysis filters.The generations of scaling and wavelet functions pertaining to these structures are also conducted in this paper. The proposed designs are implemented on Spartan-3E FPGA kit for one and three wavelet levels. To accelerate the hardware implementations and make them less-complex on an FPGA, the filter coefficients are implemented in a multiplierless manner after representing them as sum-and-difference-of-powers-of-two (SPT). Multiplications are then achieved only by shift and add.

This paper is organized as follows: Section II discusses the theory of bireciprocal lattice wave digital filters and reviews the design and realization of IIR filter banks. In section III, the proposed design method for $9^{th}$ order linear-phase IIR wavelet filter bank with perfect reconstruction property is described and the corresponding scaling and wavelet functions after five-level analysis banks are generated. The comparison between biorthogonal FIR and the designed orthogonal IIR filters are also included. Matlab programming is used in section IV to verify the results and to estimate a suitable coefficient's wordlength to work with. In section V, the descriptions of the FPGA implementations are given and the obtained results are displayed. A comparative study is illustrated in section VI. Finally, section VII concludes this paper.

## II. Background Theory

The wave digital filter is one of the structures of the IIR digital filters [5]. It possess a number of notable advantages in comparison to other IIR filter structures. Their low sensitivity, good round-off noise characteristics,optimal scaling and wide dynamic range lead to short wordlengths implementations [6]. In other words, it is possible to represent filter coefficients utilizing only few bits. This could allow for decreasing the size of applied multipliers or even replacing them by shift and add operations [2]. Therefore this kind of digital filter becomes more popular to be implemented into many varieties of integrated

circuits. A bireciprocal Lattice Wave digital filter (BLWDF), is a special form of lattice wave digital filters (LWDFs), that reduces the number of adaptors under certain conditions and can also be used as a base for decimation and interpolation filters. In BLWDF transfer functions, numerators are polynomials in $z^{-2}$.This reduces their implementation complexity. It also increases the throughput, compared to the same order LWDF implementations [7]. So, BLWDFs conducted in this paper, represent the most efficient family of IIR filters and are therefore of great interest.

As shown in Fig. 1, the low pass transfer function of BLWDF can be written as

$$H_o(z) = \frac{1}{2}[A_o(z^2) + z^{-1}A_1(z^2)] \quad \ldots(1)$$

where $A_o(z^2)$ and $A_1(z^2)$ are all-pass functions and can be expressed respectively, as [8]

$$A_0(z^2) = \prod_{i=2,4,..}^{(N+1)/2} \frac{\alpha_i + z^{-2}}{1+\alpha_i z^{-2}} \quad \ldots(2)$$

$$A_1(z^2) = \prod_{i=3,5,..}^{(N+1)/2} \frac{\alpha_i + z^{-2}}{1+\alpha_i z^{-2}} \quad \ldots(3)$$

where $\alpha_i$'s are the all-pass sections coefficients and N is the $H_o(z)$ filter order.

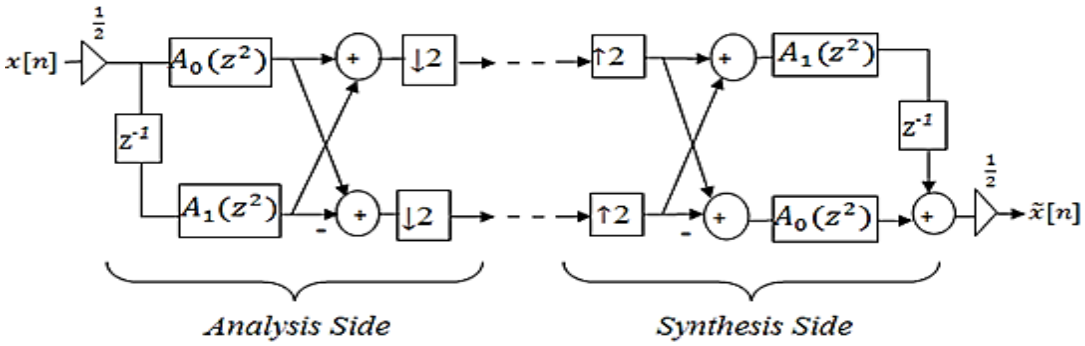


*Fig. 1 Polyphase realization of the IIR wavelet filter bank.*

The two-channel quadrature mirrorfilter (QMF) bank structure is a parallel connection of two all-pass subfilters (PCAS) [9]. The aliasing error and amplitude distortion can be eliminated by representing the QMF bank with polyphase structure [10]. Figure 1 shows a two channel all-pass filter based IIR QMF banks with polyphase realization [11]. Because the all-pass filters cannot have exact linear-phase, the QMF banks may have phase distortion [12].

To remove this phase distortion and to achieve a perfect reconstruction condition [3], a branch-interchange method is applied in the analysis side of the bank and the two all-pass sections in the synthesis side are made as function of $z^{-1}$ instead of $z$ [13]. Furthermore, in Fig.1, the filtering by 2nd order all-pass filters followed by downsampling is equivalent to having downsampling first, followed by the 1st order all-pass filters [14]. The resulting stable and efficient linear-phase filter bank (FB) structure is shown in Fig. 2.

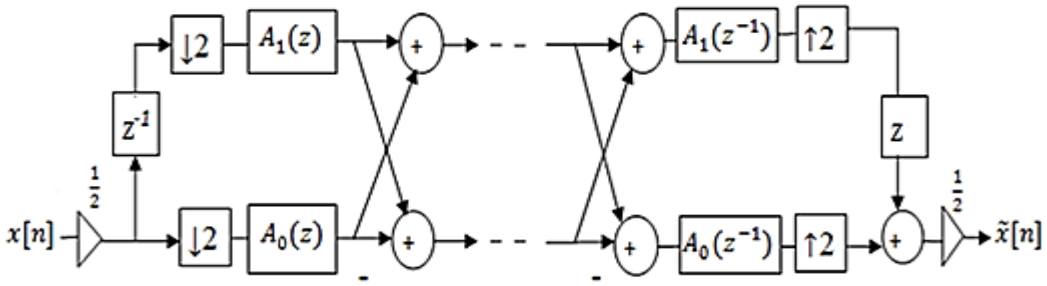


*Fig. 2 An alternative stable and efficient structure offering no phase distortion.*

The transfer function of $A_0(z)$ and $A_1(z)$ in Fig. 2 can be expressed as follows:

$$A_0(z) = \prod_{i=2,4,..}^{(N+1)/2} \frac{\alpha_i + z^{-1}}{1+\alpha_i z^{-1}} \quad \ldots(4)$$

and

$$A_1(z) = \prod_{i=3,5,..}^{(N+1)/2} \frac{\alpha_i + z^{-1}}{1+\alpha_i z^{-1}} \quad \ldots(5)$$

Let $H_0(z)$ and $H_1(z)$ denote the transfer functions of the low-pass and high- pass filter of the analysis part of the two-channel QMF bank. Also let $G_0(z)$ and $G_1(z)$ denote the transfer functions of the low-pass and high-pass filters of the synthesis part. By choosing transfer functions to satisfy thefollowing conditions: $H_1(z) = H_0(-z)$, $G_0(z) = H_0(z^{-1})$and$G_1(z) = H_1(z^{-1})$, then the filter bank will possess both perfect reconstruction and orthonormality properties [15]. Analysis filters $H_0(z)$ and $H_1(z)$ can respectively, be written thenfor the low-pass side as

$$H_o(z) = \frac{1}{2}[A_o(z) + z^{-1}A_1(z)] \quad \ldots(6)$$

and for high-pass side as

$$H_1(z) = \frac{1}{2}[A_o(z) - z^{-1}A_1(z)] \quad \ldots(7)$$

## III. The Pproposed Design For Linear-Phase IIR PR Wavelet FBS

The design procedure presented here is based on placing poles and zeros judiciously in the z-plane, to obtain IIR filter coefficients such that the resulting filter has the desired frequency response which is whose characteristics are between IIR Butterworth and Daubechies filters (intermediate filters).The half band filter's poles are placed on an imaginary axis of the complex z-plane, where one of them is placed at the origin and the remaining conjugate complex pole pairs are located between $e^{-j\pi}$ and $e^{j\pi}$. All zeros of such filters are located on the unit circle, where seven of them are placed at z = -1 for 9$^{th}$ order filter to obtain maximally flat filter which is generating regular wavelets with maximum number of vanishing moments, the remaining two zeros are required to locate on the unit circle in order to obtain the best frequency selectivity [16]. However, for a given order filter, regularity and frequency selectivity some what contradict each other [17]. For this reason, the design of the intermediate filter that has the best possible frequency selectivity for a given flatness condition is considered.

Linear-phase and orthonormality are not mutually exclusive properties for IIR filter banks. To accomplish both properties, the impulse responses of the synthesis bank filters must be the time-reversed versions of the corresponding analysis filters. If the IIR analysis filter bank uses causal filters, then the synthesis has anticausal filters [18].

## A. 9th order linear-phase intermediate IIR filter design

The proposed filter is shown in Fig. 3. It has nine zeros and nine poles. The values of these poles and zeros can be found out depending on the desired frequency response that is shown in Fig. 4.

The transfer function of such IIR filter depends on the positions of its poles and zeros as in Fig. 3. Such transfer function is given by

$$H(z) = \frac{k[(z+1)^7[(z+a)^2+b^2]]}{z(z^2+\alpha^2)(z^2+\beta^2)(z^2+\sigma^2)(z^2+\gamma^2)} \quad \ldots (8)$$

where $a$, $b$, $\alpha$ , $\beta$ ,σ and γ are constants less than 1, as shown in Fig. 3, with $k$ as amagnitude scaling factor. Equation (8) can be factorized and reordered as

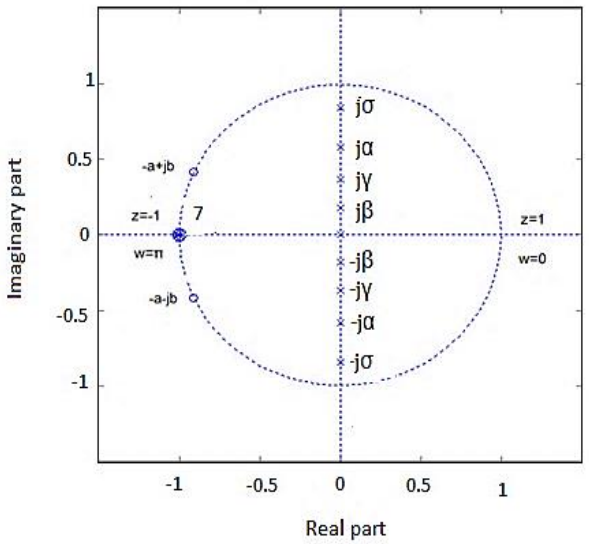


Fig. 3 Pole-zero plot for 9th order intermediate IIR half-band filter

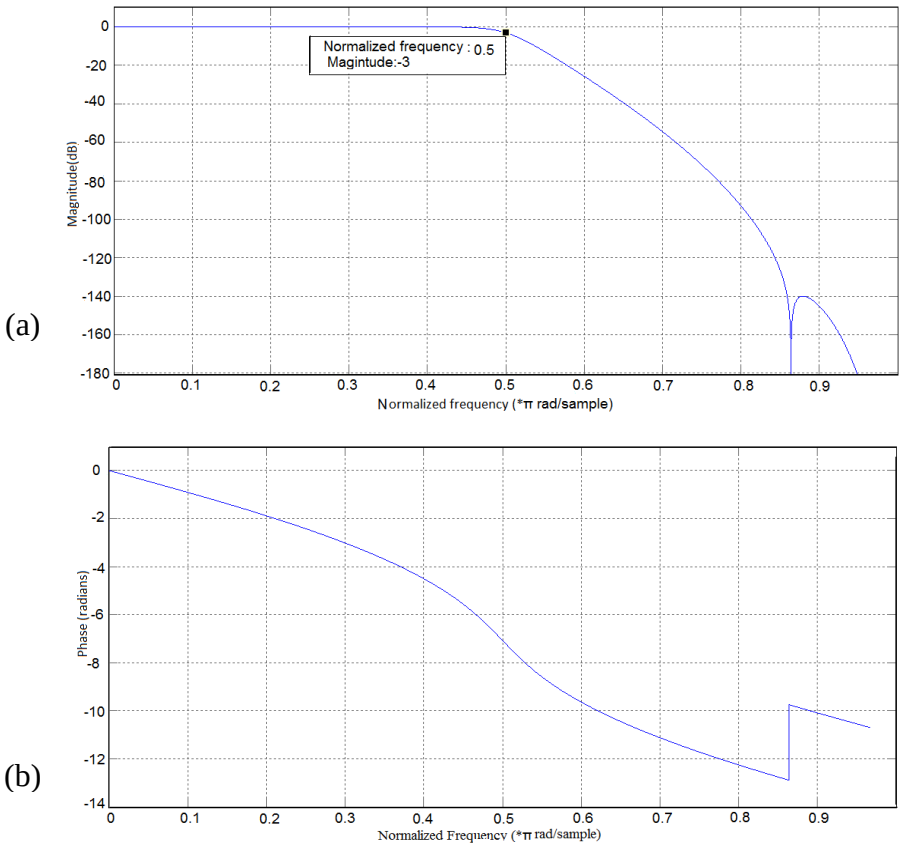


*Fig. 4 Frequency response for9th order intermediate IIR half-band filter.*
(a)*Magnitude response* (b) *Phase response.*

$$H(z)=\frac{\begin{array}{c}k[z^9+(2a+7)z^8+(a^2+b^2+14a+21)z^7+(7a^2+7b^2+42a+35)z^6\\+(21a^2+21b^2+70a+35)z^5+(35a^2+35b^2+70a+21)z^4\\+(35a^2+35b^2+42a+7)z^3+(21a^2+21b^2+14a+1)z^2\\+(7a^2+7b^2+2a)z+(a^2+b^2)]\end{array}}{\begin{array}{c}z^9+(\alpha^2+\beta^2+\gamma^2+\sigma^2)z^7+(\gamma^2\sigma^2+\beta^2\gamma^2+\beta^2\sigma^2+\alpha^2\gamma^2+\alpha^2\sigma^2+\alpha^2\beta^2)z^5+(\beta^2\gamma^2\sigma^2+\\\alpha^2\gamma^2\sigma^2+\alpha^2\beta^2\gamma^2+\alpha^2\beta^2\sigma^2)z^3+(\alpha^2\beta^2\gamma^2\sigma^2)z\end{array}} \quad \ldots(9)$$

It can be seen that (9) is expressed as a function of $z$. In order to be used in terms of $z^{-1}$, both numerator and denominator of (9) can be multiplied by $z^{-9}$, yielding

$$H(z)=\frac{\begin{array}{c}k[1+(2a+7)z^{-1}+(a^2+b^2+14a+21)z^{-2}+(7a^2+7b^2+42a+35)z^{-3}\\+(21a^2+21b^2+70a+35)z^{-4}+(35a^2+35b^2+70a+21)z^{-5}\\+(35a^2+35b^2+42a+7)z^{-6}+(21a^2+21b^2+14a+1)z^{-7}\\+(7a^2+7b^2+2a)z^{-8}+(a^2+b^2)z^{-9}]\end{array}}{\begin{array}{c}1+(\alpha^2+\beta^2+\gamma^2+\sigma^2)z^{-2}+(\gamma^2\sigma^2+\beta^2\gamma^2+\beta^2\sigma^2+\alpha^2\gamma^2+\alpha^2\sigma^2+\alpha^2\beta^2)z^{-4}+(\beta^2\gamma^2\sigma^2+\\\alpha^2\gamma^2\sigma^2+\alpha^2\beta^2\gamma^2+\alpha^2\beta^2\sigma^2)z^{-6}+(\alpha^2\beta^2\gamma^2\sigma^2)z^{-8}\end{array}} \quad \ldots(10)$$

Finding the transfer function of such 9th order filter means that the design of an intermediate IIR filter has been accomplished. The corresponding IIR filter can be implemented on BLWDF bases as a parallel connection of two all-pass IIR sections. By Gazsi method [19], that uses an alternative pole technique as illustrated in Fig. 5, the transfer functions of the two all-pass sections $A_0(z^2)$ and $A_1(z^2)$in (1) can then be derived. In Fig. 5, the poles of the region $R_1$ can formulate the transfer function of the all-pass section $A_0(z^2)$ and the poles of the region $R_2$ can formulate the transfer function of the all-pass section $A_1(z^2)$. The pole at the origin represents the delay element $z^{-1}$ in (1).

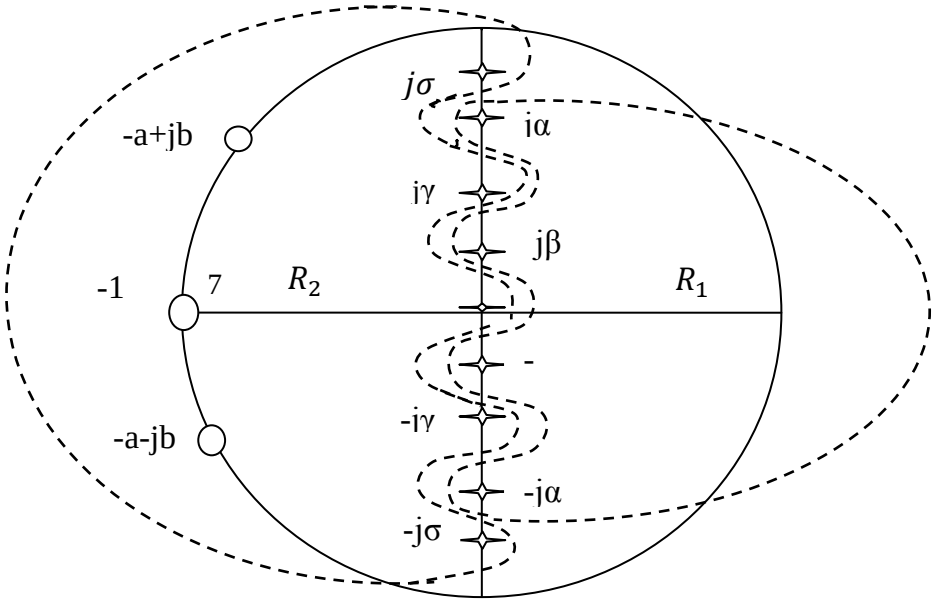


*Fig. 5 9th order alternative pole technique.*

So,

$$A_0(z^2) = \frac{z^{-4}+(\alpha^2+\beta^2)z^{-2}+\alpha^2\beta^2}{\alpha^2\beta^2 z^{-4}+(\alpha^2+\beta^2)z^{-2}+1} \quad \ldots(11)$$

$$A_1(z^2) = \frac{z^{-4}+(\sigma^2+\gamma^2)z^{-2}+\sigma^2\gamma^2}{\sigma^2\gamma^2 z^{-4}+(\sigma^2+\gamma^2)z^{-2}+1} \quad \ldots(12)$$

Substituting (11) and (12) in (1) to form the low-pass transfer function of BLWDF as

$$H_0(z) = \frac{1}{2}\left(\frac{z^{-4}+(\alpha^2+\beta^2)z^{-2}+\alpha^2\beta^2}{\alpha^2\beta^2 z^{-4}+(\alpha^2+\beta^2)z^{-2}+1} + z^{-1}\frac{z^{-4}+(\sigma^2+\gamma^2)z^{-2}+\sigma^2\gamma^2}{\sigma^2\gamma^2 z^{-4}+(\sigma^2+\gamma^2)z^{-2}+1}\right) \quad \ldots(13)$$

The design $A_0(z^2)$of and $A_1(z^2)$ is illustrated in the Appendix. Using the equations (A14) and (A15) in such Appendix, the resulting intermediate IIR $9^{th}$ order *BLWDF* low-pass transfer function depending on (A1) can be written as

$$H_0(z) = \frac{\begin{matrix}0.0055+0.04851z^{-1}+0.191z^{-2}+0.4411z^{-3}+0.6582z^{-4}\\ +0.6582z^{-5}+0.4411z^{-6}\\ +0.191\,z^{-7}+0.04851z^{-8}+0.0055z^{-9}\end{matrix}}{1+1.219z^{-2}+0.4235z^{-4}+0.04548z^{-6}+0.001067z^{-8}} \quad \ldots(14)$$

The corresponding transfer function of the high-pass filter can then be given by

$$H_1(z) = \frac{\begin{matrix}0.0055-0.04851z^{-1}+0.191z^{-2}-0.4411z^{-3}+0.6582z^{-4}\\ -0.6582z^{-5}+0.4411z^{-6}\\ -0.191\,z^{-7}+0.04851z^{-8}-0.0055z^{-9}\end{matrix}}{1+1.219z^{-2}+0.4235z^{-4}+0.04548z^{-6}+0.001067z^{-8}} \quad \ldots(15)$$

As can be seen from Fig. 4, the main drawback of IIR filter is the non-linear-phase response. To obtain linear-phase IIR wavelet filters, the structure in Fig. 2 is used, where $A_0(z)$ and $A_1(z)$ are

$$A_0(z) = \frac{z^{-2}+0.372796534z^{-1}+0.011}{0.011z^{-2}+0.372796534z^{-1}+1} \quad \ldots(16)$$

and

$$A_1(z) = \frac{z^{-2}+0.846151744z^{-1}+0.097}{0.097z^{-2}+0.846151744z^{-1}+1} \quad \ldots(17)$$

The totol phase response of upper branch ( low pass) is shown in Fig. 6.

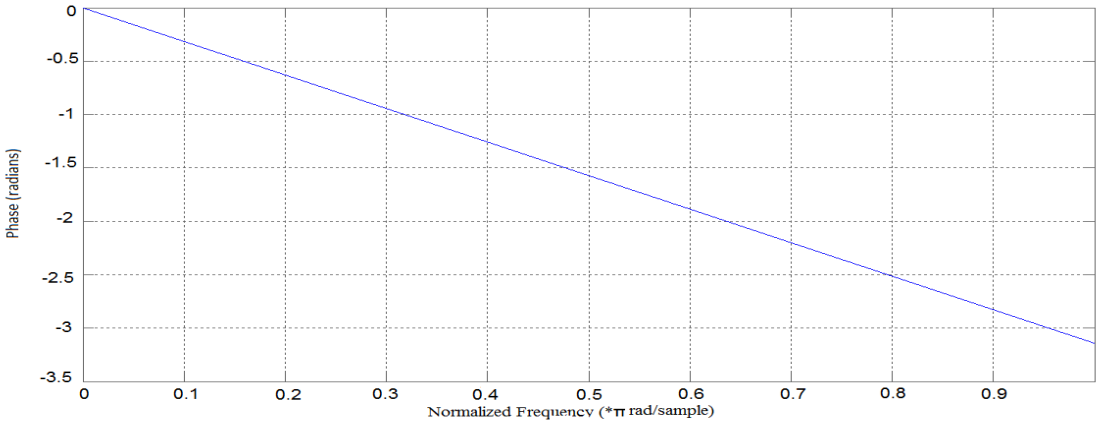


Fig. 6 Totol linear-phase response for $9^{th}$ order intermediate IIR half-band filter (low pass).

## B. Generations of scaling and wavelet functions

The basis vectors; mother wavelet and scaling functions of orthogonal wavelet transform are obtained from the iteration of the filter bank on its low-pass branch [20]. A scaling function is used to approximate an input signal at different levels of approximation. Each approximation is differed by a factor of two from the approximation at the nearest neighboring level. It should be noted that wavelet function is a type of scaling function [8], [21]. Iteration of filter bank generates equivalent band-pass filters of the form [20].

$$\Psi^i(z) = H_0(z)H_0(z^2)H_0(z^4) \dots \dots . H_0\left(z^{2^{i-2}}\right) H_1\left(z^{2^{i-1}}\right) \quad \dots (18)$$

Letting $i \to \infty$ gives the "mother wavelet" $\psi(t)$:

$$\psi(t) = \lim_{n\to\infty} \psi^i{}_{\lfloor 2^i t \rfloor} \quad \dots (19)$$

where $\psi^i[n]$ is the impulse response of $\Psi^i(z)$. The impulse response $\phi^i[n]$ of the equivalent low-pass filters of the form

$$\emptyset^i(z) = H_0(z)H_0(z^2)H_0(z^4) \dots \dots . H_0\left(z^{2^{i-2}}\right) H_0\left(z^{2^{i-1}}\right) \quad \dots (20)$$

is referred to as scaling function after $i$ iterations.

In this section, a five-level orthogonal IIR wavelet filter bank of the type shown in Fig.7. is proposed. It is realized by intermediate IIR filter pairs for the approximate generation of the corresponding wavelet (mother wavelet) and scaling functions.The mother wavelet and scaling functions can be generated after five iterations of the analysis filter banks on its low-pass branch. Iterations of the bank generate equivalent band-pass filter of the form

$$\Psi(z) = H_0(z)H_0(z^2)H_0(z^4)H_0(z^8)H_1(z^{16}) \quad \dots (21)$$

The impulse response of (21) is referred to as mother wavelet *ψ(n)*, while the impulse response of the eqivalent low-pass filter given by the form

$$\emptyset(z) = H_0(z)H_0(z^2)H_0(z^4)H_0(z^8)H_0(z^{16}) \quad \dots (22)$$

is referred to as scaling function *Ø(n).*

When all-pass IIR filter sections $A_0(z)$ and $A_1(z)$ in Fig. 7 are realized as 9th orders BLWDFs and the Dirac impulse signal is employed as input signal to the system, the output signals will represent the corresponding wavelet and scaling functions. These functions are shown in Fig. 8. They are generated after five iterations of the analysis filter bank on its low-pass branch according to (21) and (22), respectively.

Figure 7 with the aid of wavelet and scaling functions of Fig. 8 show how the DWT represents the input signal as shifted and scaled versions of the wavelet and scaling functions. Since an impulse function representation is used, the wavelet function appears in the"High wave" signals, while the scaling function appears in the''Low wave" signals.

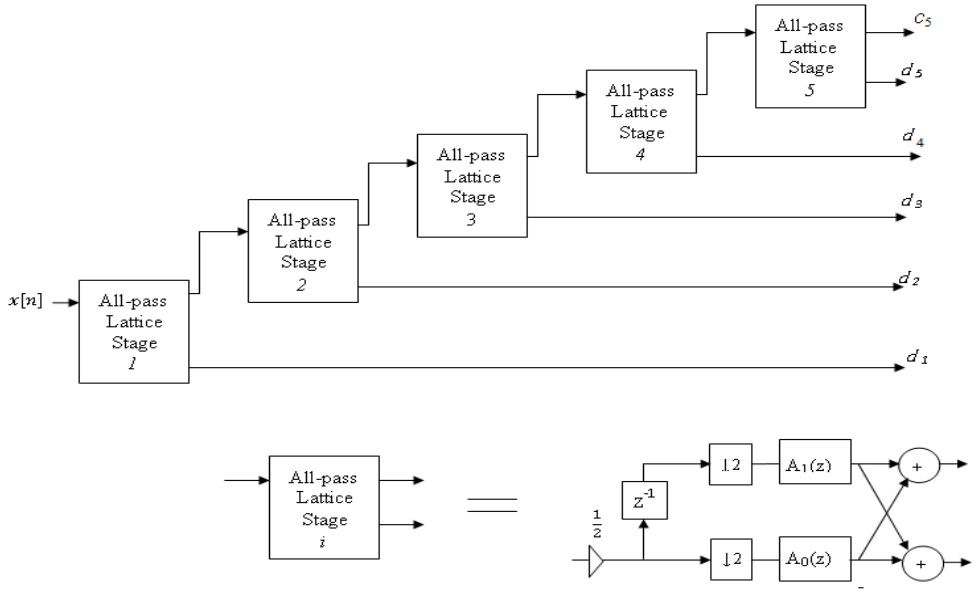


*Fig. 7 Five-level wavelet filter bank based on efficient BLWDF realization: Analysis part.*

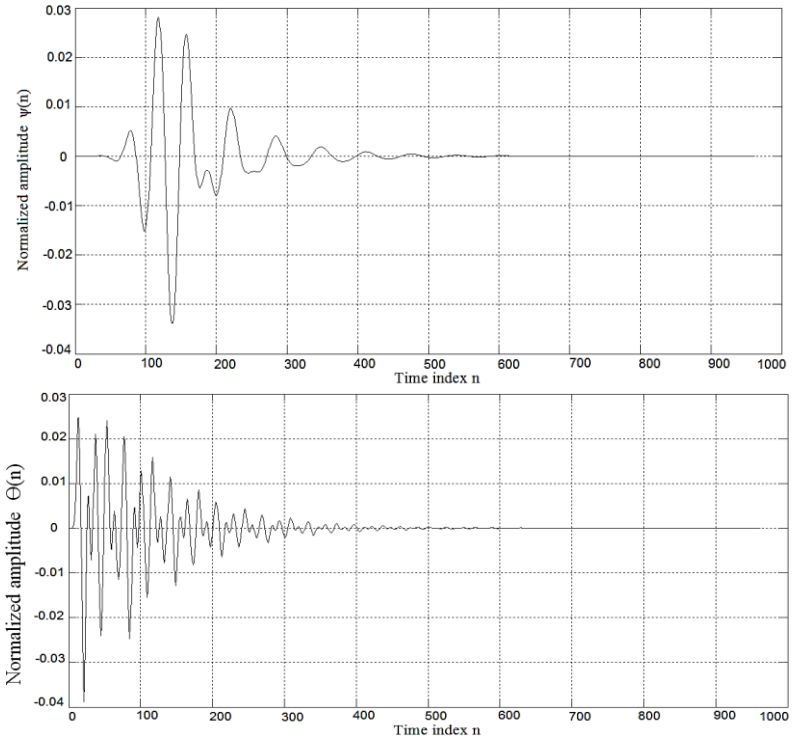


Fig. 8 9th order BLWDF bank: (a) wavelet function. (b) scaling function.

## C. Frequency response of 9th order intermediate IIR versus Biorthogonal 9/7 DWT filters

The frequency response of the designed filter is compared with those of the lifting scheme implementations of Bio. 9/7 wavelet filter bank in *Refs.* [22] & [23]. Half-band filters in wavelet transform using 9th order BLWDF possess superior band discriminations and perfect

roll-off frequency characteristics as compared to their Bio. 9/7 wavelet FIR counterparts (see Fig. 9). In addition, the biorthogonal wavelets with different number of coefficients in the low-pass and high-pass filters increase the number of operations and the complexity of the design [24].

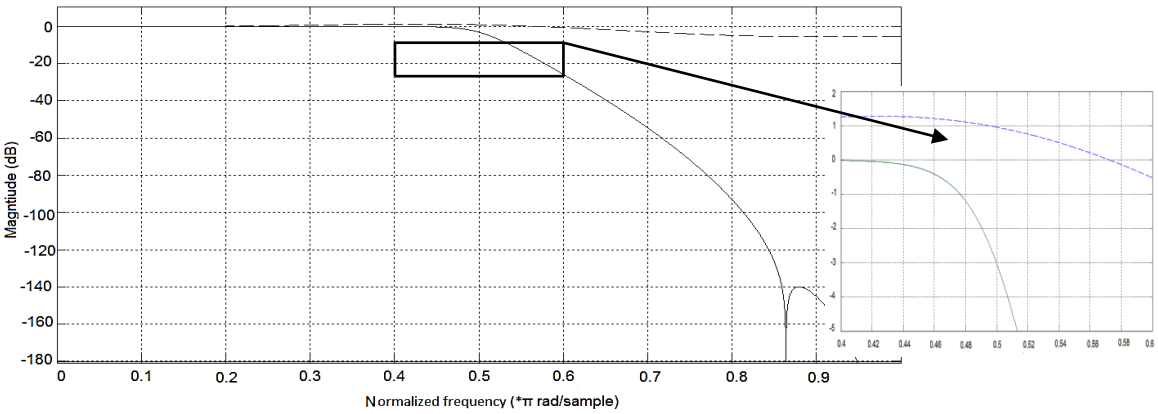


Fig. 9 Magnitude responses of $9^{th}$order low-pass BLWDWFs and low-pass Biorthogonal 9/7 DWT.

## IV. Quantizations of Filter Coefficients

Filter coefficients are quantized before implementation in fast hardware. This may change the frequency response of the filter. The filter coefficients are quantized such that the filter bank properties are preserved. This is accomplished by the right selection of wordlengths for these coefficients. In order to select a sufficient wordlength, the proposed filter should be designed according to the application (Gray scale image). Matlab programs are used to find the minimum wordlength of the BLWDF coefficients for acceptable PSNR and SNR values which are considered to be about 30 dB,correlation coefficient has value close to one, and magnitude and phase responses a of the quantized filters are closely approximate the magnitude and phase responses of the unquantized filters. This wordlength is found to be 6 bits as indicated by the PSNR readings taken for the designed filter banks using a group of gray scale test images and minimum error value between two magnitude and phase responses. Figure 10 shows the magnitude responses for quantized low-pass filter. Thus BLWDF coefficients after quantization are $\alpha^2 = 0.34375$ , $\beta^2 = 0.03125$, $\sigma^2 = 0.703125$ and$\gamma^2 = 0.140625$.

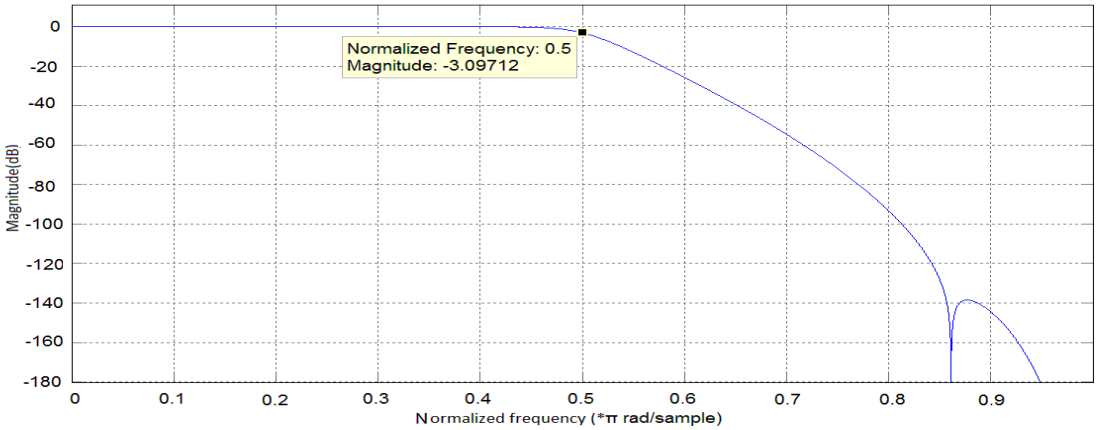


Fig. 10 Magnitude response for quantized filter.

## V. FPGA Implementations

The proposed design is described first with VHDL language. Then an FPGA device is used to implement the filter design. That device is a 500,000-gate Xilinx Spartan-3E XC3S500E in a 320-ball Fine-Pitch Ball Grid Array package (XC3S500EFG320).

### A. Implementation of one-level analysis *FBs*

An efficient hardware implementation of the BLWDF bank structure (shown in Fig. 2) with a 9th order discrete wavelet transform can be accomplished using number of Processing Elements (*PEs*). Each PE in Fig. 11 is a generic term that refers to a hardware element that executes a stream of instructions included in a 1st order all-pass section. For example, *PE-A* and *PE-B* represent the two processing elements that construct the 1st order all-pass section $A_0(z)$. The functions of *PE-A* and *PE-B* can, respectively be represented the following two difference equations:

$$y_1[n] = \alpha\, x_{even}[n] + x_{even}[n-1] - \alpha\, y_1[n-1] \quad \ldots(23)$$

$$y_2[n] = \beta\, y_1[n] + y_1[n-1] - \beta\, y_2[n-1] \quad \ldots(24)$$

where

$x_{even}$ represents the even pixels of the input image which also represents the input to *PE-A*.
$y_1[n]$ represents the output of *PE-A* which also represents the input to *PE-B*.
$y_2[n]$ represents the output of *PE-B*.
$\alpha$ represents the coefficient of *PE-A*, *i.e.*, the first part of all-pass filter $A_0(z)$.
$\beta$ represents the coefficient of *PE-B*, *i.e.*, the second part of all-pass filter $A_0(z)$.

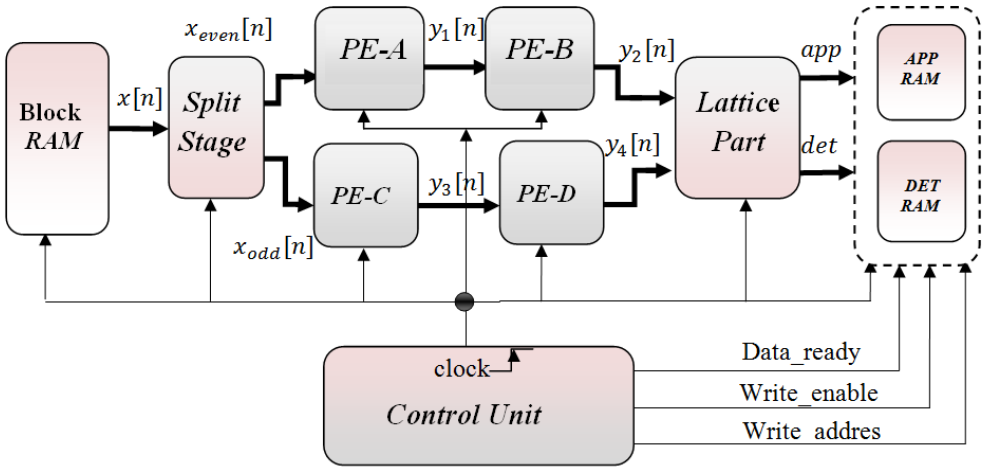


Fig. 11 Structure of one-level wavelet transform analysis side using 9th order BLWDF.

The FPGA device utilization summary for analysis side is illustrated in Table1.

Table 1 : Device utilization summary for one-level analysis side.

| | |
|---|---|
| Device utilization summary: | |
| Selected Device : 3s250evq100-4 | |
| Number of Slices: | 160 out of 4656 3% |
| Number of Slice Flip Flops: | 115 out of 9312 1% |
| Number of 4 input LUTs: | 249 out of 9312 2% |
| Timing Summary: | |
| Speed Grade: -4 | |
| Minimum period: 12.889ns | (MaximumFrequency: 77.586MHz) |
| Maximum output required time after clock: 4.283ns | |

## B. Implementation of three-level analysis *FBs*

After designing one-level analysis side structures depending on 9th order *BLWDF* as wavelet filters. They can be used to construct three-level analysis filter banks structures for such *DWT* using pipeline implementation. The block diagram of the proposed analysis side scalable structure for three-level *DWT* is shown in Fig. 12. The main units in the structure are the Processing Elements (PEs). Each PE consists of one-level analysis filter bank of the same 9th order BLWDF type shown in Fig. 11. Therefore, the PE structure depends on the chosen filter, the filter order and the selected structure of the filter banks. The FPGA device utilization summary for three-levelanalysis side is illustrated in Table 2.

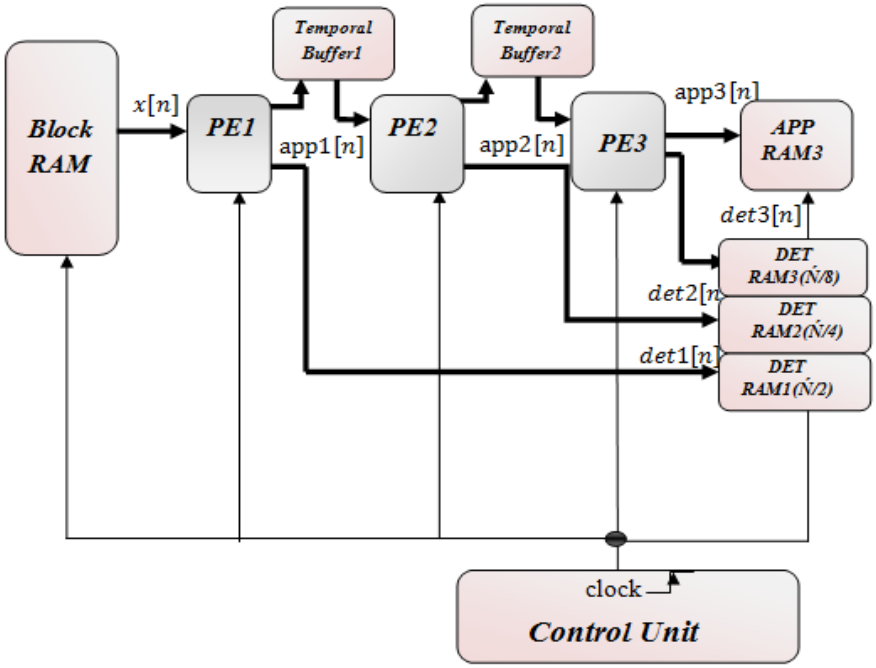


Fig. 12 Structure of three-level wavelet transform analysis side.

Table 2: Device utilization summary forthree-level analysis side.

| | | | | |
|---|---|---|---|---|
| Device utilization summary: | | | | |
| Selected Device : 3s250evq100-4 | | | | |
| Number of Slices: | 618 | out of | 4656 | 13% |
| Number of Slice Flip Flops: | 518 | out of | 9312 | 5% |
| Number of 4 input LUTs: | 886 | out of | 9312 | 9% |
| Timing Summary: | | | | |
| Speed Grade: -4 | | | | |
| Minimum period: 14.078ns (Maximum Frequency: 71.033MHz) | | | | |
| Maximum output required time after clock: 4.283ns | | | | |

## C. Implementation of one-level synthesis filter bank

The two parallel all-pass filters used in this section are $A_0(z^{-1})$, with processing elements *PEr-A* and *PEr-B*, and $A_1(z^{-1})$ ,with processing elements *PEr-C* and *PEr-D*, as shown in Fig. 13. These filters can be implemented as in $A_0(z)$ and $A_1(z)$ all-pass filters, respectively, by reversing the inputs and outputs of these filters using the last in first out (LIFO) register [18] as shown in Fig. 14. This leads to an overall wavelet reconstructed signal with exact linear phase. The FPGA device utilization summary for one-level synthesis side is illustrated in Table 3.

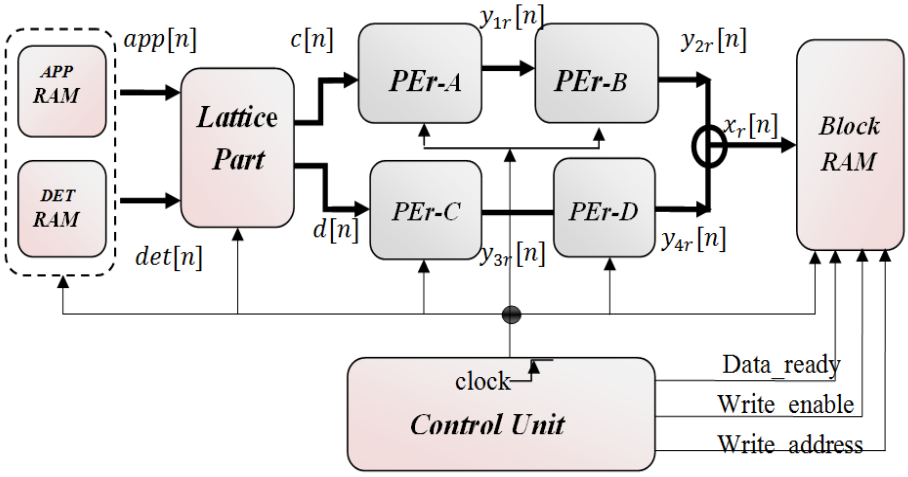


Fig. 13 Structure of one-level wavelet transform synthesis side using 9 th order BLWDF.

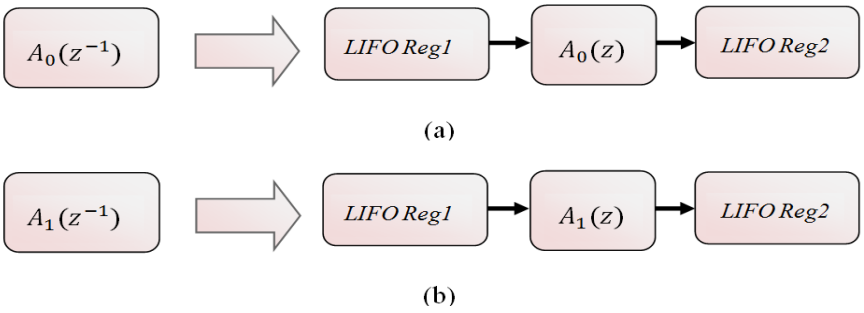


*Fig. 14 (a) Implementation of the transfer function $A_0(z^{-1})$.*
*(b) Implementation of the transfer function $A_1(z^{-1})$.*

Table 3: Device utilization summary for one-level synthesis side.

| |
|---|
| Device utilization summary:<br>Selected Device : 3s250evq100-4<br>Number of Slices: 188 out of 4656 4%<br>Number of Slice Flip Flops: 145 out of 9312 1%<br>Number of 4 input LUTs: 259 out of 9312 2% |
| Timing Summary:<br>Speed Grade: -4<br>Minimum period:14.029ns (Maximum Frequency: 71.281MHz)<br>Maximum output required time after clock: 4.283ns |

## D. Implementation of three-level synthesis filter bank

The wavelet filters constructed from 9th order *BLWDF* for one-level synthesis side structure (shown in Fig. 13) can also be used for three-level synthesis side filter banks structure of DWTas shown in Fig. 15, where the main processing element that refers to one-level synthesis side filter bankis *PEr*. The *PEr* structure depends on the chosen filter.The FPGA device utilization summary for three-level synthesis side is illustrated in Table 4.

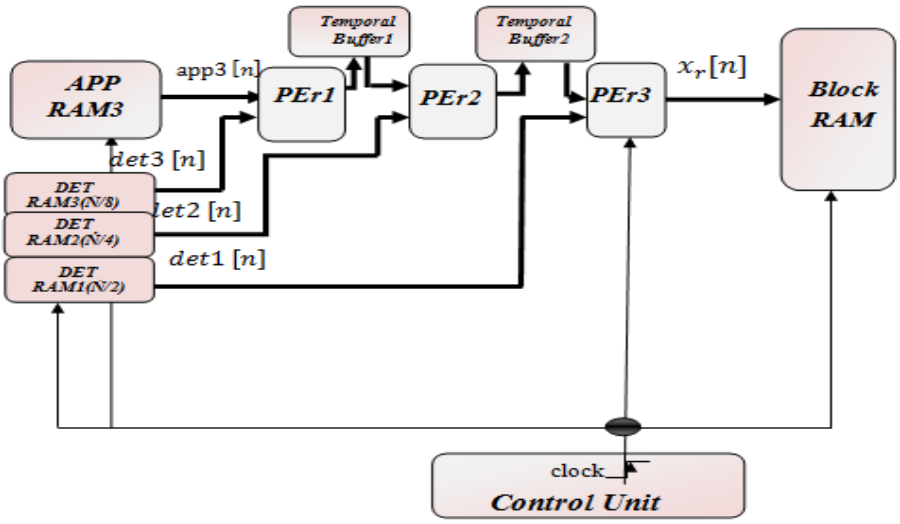


*Fig. 15 Structure of three-level wavelet transform synthesis side.*

*Table 4: Device utilization summary for three-level synthesis side.*

| |
|---|
| Device utilization summary:<br>Selected Device : 3s250evq100-4<br>Number of Slices: 626 out of 4656 13%<br>Number of Slice Flip Flops: 529 out of 9312 5%<br>Number of 4 input LUTs: 799 out of 9312 8% |
| Timing Summary:<br>Speed Grade: -4<br>Minimum period:14.030ns (Maximum Frequency: 71.276MHz)<br>Maximum output required time after clock: 4.283ns |

## VI. A Comparative Study

A comparison between the implementation of the proposed design of the $9^{th}$ order intermediate *IIR* wavelet filter bank and that of biorthogonal 9/7 lifting scheme wavelet structure in *Ref.* [23] is made using Spartan-3E FPGA device. This comparison is shown in Table 5.

*Table 5: Comparsion between the proposed $9^{th}$ order IIR wavelet FB and Bio. 9/7 lifting scheme wavelet structure.*

| *Wavelet Structure* | *Analysis/ Synthesis* | *Resource* | *Used* | *Available* | *Utilizatior ratio* |
|---|---|---|---|---|---|
| **Biorthogonal 9/7 lifting scheme in *Ref.*[23]** | ***Analysis Side Structure*** | ***Slices*** | ***45*** | ***4656*** | ***0%*** |
| | | ***Slice flip flops*** | ***39*** | ***9312*** | ***0%*** |
| | | ***4-input LUTs*** | ***87*** | ***9312*** | ***0%*** |
| | ***Synthesis Side Structure*** | ***Slices*** | ***25*** | ***4656*** | ***0%*** |
| | | ***Slice flip flops*** | ***29*** | ***9312*** | ***0%*** |
| | | ***4-input LUTs*** | ***44*** | ***9312*** | ***0%*** |
| ***The proposed* $9^{th}$ order intermediate *IIR* wavelet filter bank** | ***Analysis Side Structure*** | ***Slices*** | ***160*** | ***4656*** | ***3%*** |
| | | ***Slice flip flops*** | ***115*** | ***9312*** | ***1%*** |
| | | ***4-input LUTs*** | ***249*** | ***9312*** | ***2%*** |
| | ***Synthesis Side Structure*** | ***Slices*** | ***188*** | ***4656*** | ***4%*** |
| | | ***Slice flip flops*** | ***145*** | ***9312*** | ***1%*** |
| | | ***4-input LUTs*** | ***259*** | ***9312*** | ***2%*** |

Table 5 indicates that the utilization ratios of the proposed filter bank are of the same order of the Bio. 9/7 lifting scheme in *Ref.* [23], while the magnitude response of the proposal filter bank is more selective ( see Fig. 9), since it contains IIR filters.

## VII. Conclusions

Linear phase $9^{th}$ order IIR wavelet filter bank utilizing bireciprocal lattice wave digital filters (BLWDFs) has been designed and realized by all-pass filters. Filter coefficients has been quantized then realized in a multiplierless manner taking into account the low-coefficient sensitivity property of these wave structures.The resulting coefficients can be achieved by shift and add processes only highlighting a multiplierless realization. Multiplierless FPGA implementations of one- and three-level of bireciprocal lattice wave digital wavelet filter banks have been obtained with less complexity and high speed. Linear phase processing of such structures indicates their perfect reconstruction property.

It has been shown that, the resultimg less-complex high-speed implementation characterstics of the proposed $9^{th}$ order bireciprocal lattice wave discrete wavelet filter banks

are almost of the same orders of those in lifting scheme Bio. 9/7 wavelet structures in *Ref.* [24]. Moreover, Half-band filters in a wavelet transform using $9^{th}$ order BLWDF possess superior band discriminations and perfect roll-off frequency characteristics compared to those in Bio. 9/7 wavelet filters.

## References


[1] M. Estes, "The Discrete Wavelet Transform". ECE 402–Digital Signal Processing, Spring 2001.

[2] K. Kotteri, "Optimal, Multiplierless Implementations of the Discrete Wavelet Transform for Image Compression Applications", Master's Thesis, Electrical Engineering Department, Virginia Polytechnic Institute and State University, April 2004.

[3] S.B. JAW and S.C. PE I "Two-Band IIR Quadrature Mirror IIR Filter Design"Department of Electrical Engineering,National Taiwan University ,Taipei, Taiwan, Republic of China ,19th March 1990.

[4] S. Damjanović and L. Milić, "Examples of Orthonormal Wavelet Transform Implemented with IIR Filter Pairs", *The 2005 International 114 Workshop on Spectral Methods and Multirate Signal Processing– SMMSP2005*, Riga, Latvia, pp. 19 – 27, June, 2005.

[5] W. Sootkaneung, "The Design of Bit-Serial Lattice Wave Digital Filter Using FPGA", *IEEE Trans. On communication and signal processing*, No.5, pp. 559 - 563, Bnakok, 2005.

[6] R. Yousefi, M. H. Sargolzaie and S. M. Fakhraie, "Low Cost Concurrent Error Detection for Lattice Wave Digital Filters", *International Symposium on Telecommunications*, pp. 598 – 601, Tehran, Iran, August 2008.

[7] H. Johansson and L. Wanhammar, "Wave Digital Filter Structures for High-Speed Narrow-Band and Wide-Band Filtering", *IEEE Transactions on Circuits and Systems—II: analog and digital signal processing*, Vol. 46, No. 6, Sweden, June 1999.

[8] S. N. Mohammed " Lattice Wave Digital Filter Implementation of Wavelet Transform ", M. Sc. Thesis in Computer Engineering, Collage of Engineering, University of Mosul, Mosul, Iraq,2010.

[9] C.-K. Lu and S. Summerfield" Design and VLSI implementation of QMF banks" IEE Proc.-Vis. Image Signal Process., Vol. 151, No. 5, October 2004.

[10] E. Galijasevic and J. Kliewer, "on The Design of Near-Perfect-Reconstruction IIR QMF Banks Using FIR Phase-Compensation Filters", *University of Kiel, 2nd International Symposium on Image and Signal Processing and Analysis*, Pula, Croatia, pages 530-534, June 2001.

[11] S. Mitra, "*Digital Signal processing*", McGraw-Hill, New York, NY: 10020, ISBN 0-471-48422-9, 2001.

[12] C.K. Lu, M. Anderson and S. Summerfield, "Approximately Linear-Phase Design of All-pass-Based QMF Banks", *Proc. International Symposium on Digital signal processing*, pp. 56–61, London, 1996.

[13] J. M. Abdul-Jabbar, "Design Procedures for Two-Dimensional Digital Filters And Filter Banks", Ph.D. Thesis, Department of Electrical Engineering, Basrah University, Iraq, June 1997.

[14] B. M. Lutovac and M. D. Lutovac, "Design and VHDL description of Multiplierless Half-Band IIR Filter", *International Journal Electronic Communication (AEU) 56*,

Faculty of Electrical Engineering, University of Montenegro, Yugoslavia, No. 5, PP. 1-3, 2002.
[15] H. Ohlsson, "Studies on Implementation of Digital Filters with High Throughput and Low Power Consumption", M.Sc Thesis, Electrical Engineering, Linköping university, Sweden, June 2003.
[16] Xi Zhang, Toshinori Yoshikawa,and Hiroshi Jwakura, "Recursive Orthonormal Wavelet Bases with Vavishing Moments", *IEICE TRANS.Fundamentals*,VolE80-A,No.8 August 1997.
[17] Xi Zhang, Toshinori Yoshikawa"Design of orthonormal IIR wavelet Filter banks using all-pass Filters" *Department of Electrical Engineering, Nagaoka University of Technology, Nagaoka-shi, Niigata, 940-2188 Japan*,received 19 June 1998; received in revised form 22 December 1998.
[18] S. Damjanović, Lj. Milić, "A family of IIR two-band orhonormal QMF filter banks", *Serbian Journal of Electrical Engineering*, Vol. 1, No. 3, p.p. 45-56, Belgrade, September 2004.
[19] L. Gazsi, "Explicit Formulas for Lattice Wave Digital Filters", *IEEE Transaction on Circuits and Systems*, Vol. CAS-32, No. 1, PP. 68-88, 1985.
[20] S. Damjanović, Lj. Milić, T. Saramäki, "Frequency transformations in two-band wavelet IIR filter banks", The Special Session: Filter Banks – Novel Concepts and Applications, *EUROCON 2005 – The International Conference on "Computer as a Tool"*, Belgrade, Serbia and Montenegro, pp. 87 – 90, November 2005.
[21] H. Lee, "Wavelet Analysis for Image Processing", Institute of Communication Engineering, National Taiwan University, Taipei,Taiwan,ROC.Onhttp://disp.ee.ntu.edu.tw/henry/wavelet_analysis.pdf
[22] P. Getreuer, "Filter Coefficients to Popular Wavelets", May 2006.
[23] Z.Talal Abed Ali, "Two-Dimensional Discrete Wavelet Transform Architecture for JPEG2000 filters", M. Sc. Thesis in Computer Engineering, Collage of Engineering, University of Mosul, Mosul, Iraq, 2007.
[24] M. Nagabushanam and S. Ramachandran, " Design and Implementation of Parallel and Pipelined Distributive Arithmetic Based Discrete Wavelet Transform IP Core", *European Journal of Scientific Research*, ISSN 1450-216X Vol. 35, No.3, pp.378-392, 2009.

## APPENDIX

The final form of (13) can be written as

$$H_0(z) = \frac{1}{2}\left( \frac{\begin{array}{c}\alpha^2\beta^2+\sigma^2\gamma^2z^{-1}+(\alpha^2+\beta^2+\alpha^2\beta^2\sigma^2+\alpha^2\beta^2\gamma^2)z^{-2}+(\sigma^2+\gamma^2 \\ +\sigma^2\gamma^2\,\alpha^2+\sigma^2\gamma^2\,\beta^2)z^{-3} \\ +(\alpha^2\sigma^2+\alpha^2\gamma^2+\sigma^2\beta^2+\gamma^2\,\beta^2+\alpha^2\beta^2\gamma^2\sigma^2+1)z^{-4} \\ +(\alpha^2\sigma^2+\alpha^2\gamma^2+\sigma^2\beta^2+\gamma^2\,\beta^2+\alpha^2\beta^2\gamma^2\sigma^2+1)z^{-5} \\ +(\sigma^2+\gamma^2+\sigma^2\gamma^2\,\alpha^2+\sigma^2\gamma^2\,\beta^2)z^{-6}+(\alpha^2+\beta^2 \\ +\alpha^2\beta^2\sigma^2+\alpha^2\beta^2\gamma^2\,)z^{-7}+\sigma^2\gamma^2\,z^{-8}+\alpha^2\beta^2z^{-9}\end{array}}{\begin{array}{c}1+(\alpha^2+\beta^2+\gamma^2+\sigma^2)z^{-2}+(\gamma^2\sigma^2+\beta^2\gamma^2+\beta^2\sigma^2+\alpha^2\gamma^2+\alpha^2\sigma^2+\alpha^2\beta^2)z^{-4} \\ +(\beta^2\gamma^2\sigma^2+ \\ \alpha^2\gamma^2\sigma^2+\alpha^2\beta^2\gamma^2+\alpha^2\beta^2\sigma^2)z^{-6}+(\alpha^2\beta^2\gamma^2\sigma^2)z^{-8}\end{array}} \right) \quad \ldots (A1)$$

Referring to Fig. 3, the following equation can be written:

$$a^2 + b^2 = 1 \quad \ldots (A2)$$

And from Fig. 4, the magnitude response at ω = 0.5π is

$$\left|H\left(e^{j0.5\pi}\right)\right| = \frac{1}{\sqrt{2}} \quad \ldots (A3)$$

Substituting (A2) into (10), yields

$$H(Z) = \frac{\begin{matrix} k[1+(2a+7)z^{-1}+(14a+22)z^{-2}+(42a+42)z^{-3} \\ +(70a+56)z^{-4}+(70a+56)z^{-5} \\ +(42a+42)z^{-6}+(14a+22)z^{-7} \\ +(2a+7)z^{-8}+z^{-9}] \end{matrix}}{\begin{matrix} 1+(\alpha^2+\beta^2+\gamma^2+\sigma^2)z^{-2}+\left(\begin{matrix}\gamma^2\sigma^2+\beta^2\gamma^2+\beta^2\sigma^2+ \\ \alpha^2\gamma^2+\alpha^2\sigma^2+\alpha^2\beta^2\end{matrix}\right)z^{-4}+(\beta^2\gamma^2\sigma^2+ \\ \alpha^2\gamma^2\sigma^2+\alpha^2\beta^2\gamma^2+\alpha^2\beta^2\sigma^2)z^{-6}+(\alpha^2\beta^2\gamma^2\sigma^2)z^{-8} \end{matrix}} \quad \ldots (A4)$$

Also, substituting $z^{-1} = e^{-j\omega}$ in equation (A4), results in

$$H\left(e^{j\omega}\right) = \frac{\begin{matrix} k[1+(2a+7)e^{-j\omega}+(14a+22)e^{-j2\omega}+(42a+42)e^{-j3\omega} \\ +(70a+56)e^{-j4\omega}+(70a+56)e^{-j5\omega} \\ +(42a+42)e^{-j6\omega}+(14a+22)e^{-j7\omega} \\ +(2a+7)e^{-j8\omega}+e^{-j9\omega}] \end{matrix}}{\begin{matrix} 1+(\alpha^2+\beta^2+\gamma^2+\sigma^2)e^{-j2\omega}+(\gamma^2\sigma^2+\beta^2\gamma^2+\beta^2\sigma^2+\alpha^2\gamma^2+\alpha^2\sigma^2+\alpha^2\beta^2)e^{-j4\omega}+(\beta^2\gamma^2\sigma^2+ \\ \alpha^2\gamma^2\sigma^2+\alpha^2\beta^2\gamma^2+\alpha^2\beta^2\sigma^2)e^{-j6\omega}+(\alpha^2\beta^2\gamma^2\sigma^2)e^{-j8\omega} \end{matrix}} \quad \ldots (A5)$$

Using Euler formula, the magnitude response is then given by

$$\left|H\left(e^{j\omega}\right)\right| = \frac{\begin{matrix} k\{[1+(2a+7)(cos\omega+cos8\omega)+(14a+22)(cos2\omega+cos7\omega)+ \\ (42a+42)(cos3\omega+cos6\omega)+(70a+56)(cos4\omega+cos5\omega) \\ +cos9\omega]^2+[(2a+7)(sin\omega+sin8\omega)+(14a+22)(sin2\omega+sin7\omega) \\ +(42a+42)(sin3\omega+sin6\omega)++(70a+56)(sin4\omega sin5\omega) \\ +sin9\omega]^2\}^{\frac{1}{2}} \end{matrix}}{\begin{matrix} \{[1+(\alpha^2+\beta^2+\gamma^2+\sigma^2)cos2\omega+(\gamma^2\sigma^2+\beta^2\gamma^2+\beta^2\sigma^2+\alpha^2\gamma^2+\alpha^2\sigma^2+\alpha^2\beta^2)cos4\omega \\ +(\beta^2\gamma^2\sigma^2+\alpha^2\gamma^2\sigma^2+\alpha^2\beta^2\gamma^2+\alpha^2\beta^2\sigma^2)cos6\omega \\ +(\alpha^2\beta^2\gamma^2\sigma^2)cos8\omega]^2+[(\alpha^2+\beta^2+\gamma^2+\sigma^2)sin2\omega+ \\ (\gamma^2\sigma^2+\beta^2\gamma^2+\beta^2\sigma^2+\alpha^2\gamma^2+\alpha^2\sigma^2+\alpha^2\beta^2)sin4\omega+ \\ (\beta^2\gamma^2\sigma^2+\alpha^2\gamma^2\sigma^2+\alpha^2\beta^2\gamma^2+\alpha^2\beta^2\sigma^2)jsin6\omega+ \\ (\alpha^2\beta^2\gamma^2\sigma^2)sin8\omega]^2\}^{\frac{1}{2}} \end{matrix}}$$

... (A6)

By assuming initial values for *a, b,* $\alpha$ , $\beta$ ,σ and γ. The value of *k* can be obtained numerically to be equal to 0.0055, so that $H\left(e^{j0}\right) = 1$.

Substituting (A3) in (A6), yields

$$\frac{1}{\sqrt{2}} = \frac{0.124450793a}{\begin{matrix} [1-(\alpha^2+\beta^2+\gamma^2+\sigma^2)+(\gamma^2\sigma^2+\beta^2\gamma^2+\beta^2\sigma^2+\alpha^2\gamma^2+\alpha^2\sigma^2+\alpha^2\beta^2) \\ -(\beta^2\gamma^2\sigma^2+\alpha^2\gamma^2\sigma^2+\alpha^2\beta^2\gamma^2+\alpha^2\beta^2\sigma^2) \\ +(\alpha^2\beta^2\gamma^2\sigma^2)] \end{matrix}} \quad \ldots (A7)$$

Expressing *a* in terms of other variables, yields

$$a = 5.68[\,(1-(\alpha^2+\beta^2+\gamma^2+\sigma^2)+(\gamma^2\sigma^2+\beta^2\gamma^2+\beta^2\sigma^2+\alpha^2\gamma^2+\alpha^2\sigma^2+\alpha^2\beta^2)- (\beta^2\gamma^2\sigma^2+\alpha^2\gamma^2\sigma^2+\alpha^2\beta^2\gamma^2+\alpha^2\beta^2\sigma^2)+(\alpha^2\beta^2\gamma^2\sigma^2)\,] \quad \ldots (A8)$$

The filter coefficients can be calculated by identically equating (A1) to the general filter function (10), resulting in the followings:

*for the absolute terms*

$$0.5\alpha^2\beta^2 = 0.0055 \quad \ldots(A9)$$

*for $z^{-1}$terms*

$$0.5\gamma^2\sigma^2 = 0.0055(2a+7) \quad \ldots(A10)$$

*for $z^{-2}$terms*

$$0.5(\alpha^2+\beta^2+\alpha^2\beta^2\sigma^2+\alpha^2\beta^2\gamma^2) = 0.0055(14a+22) \quad \ldots(A11)$$

*for $z^{-3}$terms*

$$0.5(\sigma^2+\gamma^2+\sigma^2\gamma^2\alpha^2+\sigma^2\gamma^2\beta^2) = 0.0055(42a+42) \quad \ldots(A12)$$

*for $z^{-4}$terms*

$$0.5(\alpha^2\sigma^2+\alpha^2\gamma^2+\sigma^2\beta^2+\gamma^2\beta^2+\alpha^2\beta^2\gamma^2\sigma^2+1) = 0.0055(7a+56) \quad \ldots(A13)$$

Equations (A9) to (A13) can be solved numerically using fixed point iteration method to find out that

| | |
|---|---|
| $\alpha^2 = 0.340489311$ | $\alpha = 0.583514612$ |
| $\beta^2 = 0.032307223$ | $\beta = 0.179742102$ |
| $\sigma^2 = 0.709387198$ | $\sigma = 0.842251268208$ |
| $\gamma^2 = 0.136764546$ | $\gamma = 0.369816910303$ |
| $a^2 = 0.827596149$ | $a = 0.909723117$ |
| $b^2 = 0.17240385$ | $b = 0.415215426$ |

Substituting the above coefficient in equations (11) and(12) results in the followings:

$$A_0(z^2) = \frac{z^{-4}+0.372796534z^{-2}+0.011}{0.011z^{-4}+0.372796534z^{-2}+1} \quad \ldots(A14)$$

and

$$A_1(z^2) = \frac{z^{-4}+0.846151744z^{-2}+0.097}{0.097z^{-4}+0.846151744z^{-2}+1} \quad \ldots(A15)$$

**The work was carried out at the college of Engineering. University of Mosul**